Synthesis, Characterization, and Adsorption Studies of Nanocrystalline Aluminum Oxide and a Bimetallic Nanocrystalline Aluminum Oxide/Magnesium Oxide

ARTICLE *in* CHEMISTRY OF MATERIALS · JUNE 2002

Impact Factor: 8.35 · DOI: 10.1021/cm011590i

3 AUTHORS:

Corrie Carnes
MRIGlobal-Midwest Research Institute
11 PUBLICATIONS **751** CITATIONS
SEE PROFILE

Pramesh N Kapoor
University of Delhi
121 PUBLICATIONS **1,631** CITATIONS
SEE PROFILE

Kenneth Klabunde
Kansas State University
357 PUBLICATIONS **13,564** CITATIONS
SEE PROFILE

Synthesis, Characterization, and Adsorption Studies of Nanocrystalline Aluminum Oxide and a Bimetallic Nanocrystalline Aluminum Oxide/Magnesium Oxide

Corrie L. Carnes, Pramesh N. Kapoor, and Kenneth J. Klabunde*

Department of Chemistry, Kansas State University, Manhattan, Kansas 66506

John Bonevich

Metallurgy, NIST, Stop 8554, 100 Bureau Drive, Gaithersburg, Maryland 20899

Received November 2, 2001. Revised Manuscript Received April 25, 2002

Nanocrystals of Al_2O_3 and Al_2O_3/MgO have been produced by a modified aerogel synthesis involving the corresponding aluminum tri-*tert*-butoxide, magnesium methoxide, toluene, methanol, ethanol, and water. The resulting oxides are in the form of powders having crystallites of about 2 nm or less in dimension. These crystallites have been studied by transmission electron microscopy (TEM), and Brunauer−Emmet−Teller (BET) methods, and were found to possess high surface areas and pore volumes (800 m^2/g for Al_2O_3 and 790 m^2/g for Al_2O_3/MgO, compared to 450 m^2/g for MgO). As seen with other metal oxides, once they are produced as nanoparticles, their reactivity is greatly enhanced on a per unit surface area basis. This is thought to be due to morphological differences, whereas larger crystallites have only a small percentage of reactive sites on the surface, smaller crystallites possess much higher surface concentration of such sites per unit surface area. Elemental analysis, X-ray diffraction, and infrared spectroscopy have been used to characterize these nanoparticles, and reactions with CCl_4, SO_2, and Paraoxon have demonstrated significantly enhanced reactivity and/or capacity compared with common commercial forms of the oxide powders. A significant feature is that, by a cogellation synthesis, Al_2O_3 and MgO have been intermingled, which engenders enhanced reactivity/capacity over the pure forms of nanoscale Al_2O_3 or MgO toward a chemical warfare surrogate (Paraoxon) and an acid gas (SO_2). This serves as an example where tailored synthesis of a nanostructured formulation can yield special benefits.

Introduction

Alumina and magnesia are two of the most widely used ceramic materials, and have found use as catalysts, catalyst supports, and adsorbents and for wear resistant coatings.[1−11] Many methods for preparation of these oxides have been reported,[12−17] including mixed oxides.[18−33]

The objective of the work reported herein was to improve upon these earlier preparations by using a modified aerogel procedure, employing alcohol−toluene

(1) Lercher, J. A.; Colombier, C.; Vinek, H.; Noller, H. *Catalysis by Acids and Bases, Proceedings of an International Symposium September 25−27, 1984*; Elsevier: Amsterdam, 1985; p 25.
(2) Ozawa, S.; Nakatani, J.; Ochi, J.; Sato, M.; Ogino, Y. *Proceedings of the International Symposium on Acid−Base Catalysis, Sapporo, November 28−December 1, 1988*.
(3) Captain, D. K.; Amiridis, M. D. *J. Catal.* **1999**, *184*, 377.
(4) Beretta, A.; Piovesan, L.; Forzatti, P. *J. Catal.* **1999**, *184*, 455.
(5) Yao, Y. Y. *J. Phys. Chem.* **1965**, *69*, 11, 3930.
(6) Dua, A. K.; George, V. G.; Agarwala, R. P. *Thin Solid Films* **1988**, *165*, 163.
(7) Gallas, M. R.; Hockey, B.; Pechenik, A.; Piermarini, G. J. *J. Am. Ceram. Soc.* **1994**, *77*, 8, 2107.
(8) Mishra, R. S.; Lesher, C. E.; Mukherje, A. K. *J. Am. Ceram. Soc.* **1996**, *79*, 2989.
(9) Costa, T. M. H.; Gallas, M. R.; Benvenutti, E. V.; Jornada, J. A. H. *J. Phys. Chem. B* **1999**, *103*, 4278.
(10) Zacheis, G. A.; Gray, K. A.; Kamat, P. V. *J. Phys. Chem. B* **1999**, *103*, 2142.
(11) Gallas, M. R.; Piermarini, G. J. *J. Am. Ceram. Soc.* **1994**, *77*, 11, 2917.
(12) Chou, T. C.; Adamson, D.; Mardinly, J.; Nieh, T. G. *Thin Solid Films* **1991**, *205*, 131.
(13) Dokhale, P. A.; Sali, N. D.; Kumar, P. M.; Bhoraskar, S. V.; Rohatgi, V. K.; Bhoraskar, V. N.; Date, S. K.; Badrinarayanan, S. *Mater. Sci. Eng.* **1997**, *B49*, 18.
(14) Mamchik, A. I.; Kalinin, S. V.; Vertegel, A. A. *Chem. Mater.* **1998**, *10*, 3548.
(15) Patra, A.; Sominska, E.; Ramesh, S.; Koltypin, Y.; Zhong, Z.; Minti, H.; Reisfeld, R.; Gedanken, A. *J. Phys. Chem. B* **1999**, *103*, 3361.
(16) Wang, J. A.; Bokhimi, X.; Morales, A.; Novaro, O.; López, T.; Gómez, R. *J. Phys. Chem. B* **1999**, *103*, 299.
(17) Ramesh, S.; Sominska, E.; Cina, B.; Chaim, R.; Gedanken, A. *J. Am. Ceram. Soc.* **2000**, *83*, 1, 89.
(18) Amigó, R.; Asenjo, J.; Krotenko, E.; Torres, F.; Tejada, J. *Chem. Mater.* **2000**, *12*, 2, 573−579.
(19) Rodriguez, J. A.; Hanson, J. C.; Chaturvedi, S.; Maiti, a.; Brito, J. L. *J. Chem. Phys.* **2000**, *112*, 2, 935−945.
(20) Leroux, F.; Piffard, Y.; Ouvrard, G.; Mansot, J. L.; Guyomard, D. *Chem. Mater.* **1999**, *11*, 10, 2948−2959.
(21) Heinz, D.; Hoelderich, W. F.; Krill, S.; Boeck, W.; Huthmacher, K. *J. Catal.* **2000**, *192*, 1−10.
(22) Watanabe, H.; Koyasu, Y. *Appl. Catal., A* **2000**, 194−195, 479−485.
(23) Tada, H.; Hattori, A.; Tokihisa, Y.; Imai, K.; Tohge, N.; Ito, S. *J. Phys. Chem. B* **2000**, *104*, 19, 4585−4587.
(24) Hino, M.; Arata, K. *Appl. Catal., A* **1998**, *173*, 121−124.
(25) Watson, R. B.; Ozkan, U. S. *J. Catal.* **2000**, *191*, 12−29.
(26) Wang, C. H.; Weng, H. S. *Ind. Eng. Chem. Res.* **1997**, *36*, 7, 2537−2542.
(27) Rajagopal, S.; Grimm, T. L.; Collins, D. J.; Miranda, R. *J. Catal.* **1992**, *137*, 453.

10.1021/cm011590i CCC: $22.00
Published on Web 06/22/2002

solvent mixtures, rapid hydrolysis and gelation, and supercritical drying of solvent. This approach has been very successful for synthesis of $Mg(OH)_2$ and MgO nanocrystalline samples,[34−36] and its application for $Al(OH)_3$ and Al_2O_3 synthesis was thought to be worthy of investigation. A second major objective was to use similar approaches to prepare intimate mixtures of nanostructured Al_2O_3/MgO and determine if the chemical properties of such an intimate solid mixture would be enhanced over the separate nanostructured Al_2O_3 and MgO.

These investigations have met with some success, where very high surface area Al_2O_3 (770−810 m^2/g) and the mixed material Al_2O_3/MgO (790−830 m^2/g) have been obtained. Furthermore, the mixed product does show enhanced adsorptive activity for an acid gas (SO_2) and destructive adsorptive activity for a polar organic (Paraoxon) compared with analogous pure nanostructured Al_2O_3 or MgO. These results suggest that enhanced chemical reactivities should be attainable for a wide variety of intimately intermingled mixed oxides in nanocrystalline form.

Experimental Section

Aluminum tri-*tert*-butoxide (Aldrich), *tert*-butyl alcohol (Fisher), toluene (Fisher), absolute ethanol (Aaper Alcohol and Chemical Co.), magnesium metal (Fisher), and methanol (Fisher) were used as received. Commercially available oxides, CM−Al_2O_3 from Baker Analytical and CM−MgO from Aldrich were also used as received.

Synthesis of Nanocrystalline Aluminum Oxide (NC−Al_2O_3) by a Modified Aerogel Procedure. Under argon, 1.00 g (0.0040 mol) of aluminum tri-*tert*-butoxide was added to a 500 mL round-bottom flask. This was dissolved in a solution of 100 mL of toluene and 40 mL of *tert*-butyl alcohol to form a clear colorless solution. A solution of 0.216 mL (0.0120 mol) of distilled water in 70 mL of absolute ethanol was added dropwise to form the aluminum hydroxide gel. The reaction mixture was stirred at room temperature for 10 h and remained a colorless, soft gel. The hydroxide sol−gel was transferred to a glass liner of a Parr autoclave. The autoclave was first flushed with nitrogen and then pressurized (with nitrogen) to 100 psi. While the reaction was being stirred, the reactor was slowly heated (1 °C/min) from room temperature to 265°C, and pressure increased from 100 to 1100 psi. Once the autoclave reached 265 °C, the reactor was vented to the atmosphere, very quickly removing the solvent vapors (which took about 1 min). Next the furnace was removed and the bomb was flushed with nitrogen for 10 min to remove the remaining solvent vapors. The autoclave was allowed to cool to room temperature, yielding a fluffy, white $Al(OH)_3$, which was placed in a Schlenk tube, connected to a vacuum line, and surrounded by a furnace. The Schlenk tube was evacuated at room temperature for 1 h. Next it was slowly heated from room temperature to 500 °C while under dynamic vacuum. After the heat treatment was complete, the furnace was turned off and the Schlenk tube was allowed to cool to room temperature, while still under dynamic vacuum. After heat treatment, the aluminum oxide had a light gray color, due to a small amount of carbon formation (from pyrolysis of residual alkoxy groups).

Synthesis of High Surface Area Mixed NC−Al_2O_3/MgO. First the magnesium methoxide solution, was prepared,[17] which is briefly described here. Under argon 0.500 g (0.020 mol) of Mg that had been sandpapered, wiped clean with an acetone-wet Kimwipe, and cut into small pieces, was added to a 200 mL round-bottom flask. To the Mg was added 50 mL of methanol, and this was allowed to react while stirring overnight to form a clear colorless solution. Fifty milliliters of toluene was added to this solution, and it was allowed to stir for 2 h. In a separate 500 mL round-bottom flask, under argon, 1.00 g (0.0040 mol) of aluminum tri-*tert*-butoxide was added. This was dissolved in a solution of 100 mL of toluene, and 40 mL of *tert*-butyl alcohol to form a clear colorless solution. The alkoxide solutions were mixed to give the desired molar percentages and then hydrolyzed, with a solution containing a stoichiometric amount of distilled water in 70 mL of absolute ethanol (added dropwise). The reaction was then stirred at room temperature for 10 h. During this time the reaction mixture remains a clear colorless liquidlike gel. The hydroxide sol−gel was transferred to a glass liner of a Parr autoclave, and dried as described for the pure alumina system. Thermal conversion of aluminum hydroxide/magnesium hydroxide to aluminum oxide/magnesium oxide was carried out as described for the pure alumina system. After heat treatment, the aluminum/magnesium oxide had a light gray color.

Characterization. *Transmission Electron Microscopy (TEM).* TEM studies were carried out by adding dry ethanol to the heat-treated Al_2O_3, and sonicating this slurry for 5 min using a Branson 1210 sonicator. A drop of this slurry was then placed onto a carbon-coated copper grid. TEM experiments were performed using a Philips 201 TEM or a Philips CM12 TEM.

Brunauer−Emmet−Teller (BET). Surface area measurements were done by using BET methods. These were conducted using both Micromeritics Flowsorb II 2300 and Quantachrome NOVA 1200 instrumentation. The samples were first outgassed at the desired temperature and then allowed to cool to room temperature.

Powder X-ray Diffraction (XRD). For XRD studies the Al_2O_3 samples were heat treated under vacuum directly before being placed onto the sample holder. The instrument used was a Scintag XDS 2000 spectrometer. Cu Kα radiation was the light source used with applied voltage of 40 kV and current of 40 mA. The 2θ angles ranged from 20 to 85° with a speed of 2°/min. The crystallite size was then calculated from the XRD spectra using the Scherrer equation.

Infrared Spectroscopy (FT-IR). FT-IR was used to observe solvent removal during the heat treatment process. These experiments were conducted on an RS-1 FTIR spectrometer from Mattson with a liquid-nitrogen-cooled MCT detector. Heat-treated samples of NC−Al_2O_3 and CM−Al_2O_3 were made into KBr pellets and studied.

Thermogravimetric Analysis (TGA). TGA was used to determine the conversion of $Al(OH)_2$ to Al_2O_3 during heat treatment. These studies were conducted under a nitrogen flow. To measure the weight loss the Al_2O_3 samples were placed in a basket and heated at a rate of 10°/min from room temperature to 700 °C. The instrument used was a thermogravimetric analyzer TGA-50 from the Shimadzu Co.

Elemental Analysis. Al_2O_3 after heat treatment was transferred to glass vials, under argon atmosphere, and sent to Galbraith Laboratories for analysis. Elemental analysis was conducted for Al, C, and H. The amount of oxygen was obtained by subtracting the sum of Al, C, and H from 100.

Adsorption Studies. *Reaction of Al_2O_3* and Al_2O_3/MgO with CCl_4. These reactions were conducted in a U-tube that was connected to a gas chromatograph (GOW-MAC gas chromatograph series 580).[34] The U-tube was made of Pyrex and connected between the injector port and the column (Alltech

(28) Corma, A. *Chem. Rev.* **1995**, *95*, 559.
(29) Reddy, B. N.; Subrahmanyam, M. *Langmuir* **1992**, *8*, 2072.
(30) Kiessling, D.; Went, G.; Hagenau, K.; Schoellner, R. *Appl. Catal.* **1991**, *71*, 69.
(31) Ahlstrom-Silversand, A. F.; Odenbrand, C. U. I. *Appl. Catal.* **1997**, *153*, 157.
(32) Abello, M. C.; Gomez, M. F.; Cadús, L. E. *Ind. Eng. Chem. Res.* **1996**, *35*, 7, 2137−2143.
(33) Chi, Y.; Chuang, S. S. C. *J. Phys. Chem. B* **2000**, *104*, 19, 4673−4683.
(34) (a) Koper, O. B.; Lagadic, I.; Volodin, A.; Klabunde, K. *J. Chem. Mater.* **1997**, *9*, 2468. (b) Carnes, C. L.; Klabunde, K. J. *Langmuir* **2000**, *16*, 8, 3764−3772.
(35) (a) Stark, J. V.; Park, D. G.; Lagadic, I.; Klabunde, K. J. *Chem. Mater.* **1996**, *8*, 1904−1912. (b) Klabunde, K. J.; Stark, J.; Koper, O.; Mohs, C.; Park, D. G.; Decker, S.; Jiang, Y.; Lagadic, I.; Zhang, D. *J. Phys. Chem.* **1996**, *100*, 12142.
(36) Wagner, G. W.; Procell, L. R.; O'Connor, R. J.; Munavalli, S.; Carnes, C. L.; Kapoor, P. N.; Klabunde, K. J. *J. Am. Chem. Soc.* **2001**, *123*, 1636−1644.

Table 1. Nanocrystalline Aluminum Oxide Preparation Variables

sample no.	starting material	solvent	stirring time (h)	surface area (m^2/g)
1	aluminum triethoxide	toluene/ethanol (100 mL/40 mL)	2	352
2	aluminum triethoxide	toluene/ethanol (100 mL/40 mL)	10	385
3	aluminum isoproproxide	toluene/2-propanol (100 mL/40 mL)	2	224
4	aluminum isoproproxide	toluene/2-propanol (100 mL/40 mL)	10	243
5	aluminum tributoxide	toluene/butanol (100 mL/40 mL)	2	392
6	aluminum tributoxide	toluene/butanol (100 mL/40 mL)	10	369
7	aluminum tri-*tert*-butoxide	toluene/*tert*-butanol (100 mL/40 mL)	2	743
8	aluminum tri-*tert*-butoxide	toluene/*tert*-butanol (100 mL/40 mL)	10	810
9	aluminum tri-*tert*-butoxide	toluene/*tert*-butanol (100 mL/40 mL)	20	735
10	aluminum tri-*tert*-butoxide	toluene/*tert*-butanol (50 mL/40 mL)	10	673
11	aluminum tri-*tert*-butoxide	toluene/*tert*-butanol (150 mL/40 mL)	10	779

Chromosorb W-HP). An oxide sample (0.100 g) was placed in the U-tube between two small plugs of quartz wool. The most favorable temperatures for both reactions were found to be at 500 °C, and the U-tube was heated to this temperature. The injector port was kept at 100 °C. Injections of 2 μL of CCl_4 were made every 7 min. Any CO_2 coming off the sample, or CCl_4 that was not destroyed, was then sent via helium (20 cm^3/min) through the column (90 °C) to be separated. They were then detected by a thermal conductivity detector (120 °C) and peak areas recorded. Injections of CCl_4 were made until the oxide bed had been exhausted.

Sulfur Dioxide Adsorption. A quartz spring balance was used to measure the adsorption of SO_2 onto Al_2O_3 and Al_2O_3/MgO. The apparatus consists of a basket, which is used to hold the sample, and this is attached to a quartz spring.[35] The basket and the spring are closed within the vacuum line. The SO_2 gas tank is also attached to the vacuum line. As the SO_2 adsorbs onto the metal oxide in the basket, the weight change causes the spring to move, and this movement is noted by a telescope. Once the telescope is calibrated, it is accurate to ±0.1 mg.

Granules (100 mg) of oxides were placed into the basket on the spring balance. The samples were placed under dynamic vacuum for 1 h at room temperature. After evacuation, the vacuum line was closed to the pump and the spring position was noted. The SO_2 gas was allowed to fill the vacuum line, including the spring balance to the desired pressure. The spring position was noted over the next hour. This was followed by 100 min of evacuation to remove all physisorbed species. After the evacuation the spring position was noted again, indicating the presence of remaining strongly chemisorbed species.

Destructive Adsorption of Diethyl 4-Nitrophenyl Phosphate. A 0.100 g sample was placed into a 250 mL round-bottom flask that had been flushed with argon, 100 mL dry pentane was then added to the flask, and stirring commenced. Then 8 μL of Paraoxon was added to the flask, and ultraviolet/visible spectroscopy (SIM Aminco Milton Roy 3000 array) was used to monitor the disappearance of Paraoxon at 270 nm wavelength, by extracting samples at desired intervals. This reaction was monitored every 20 min for 3 h and then at 20 h. The powder was then filtered and FTIR was then used to detect adsorbed species on the solid. The used solid was also washed with 10 mL portions of CH_2Cl_2, and the IR spectra of the extracts showed that no adsorbed species were removed. Additional studies have been previously conducted with the actual chemical warfare agents.[36]

Results

Preparation of the Aluminum Oxide. Several experiments were conducted varying the starting materials, solvents, and stirring time, and all were found to have an effect on the surface area of the resulting sample. Some of the results are shown in Table 1.

It can be seen the best results were obtained for sample number eight, using aluminum tri-*tert*-butoxide as the starting material. The data support earlier findings that report that branched alkyl molecular precursors lead to higher surface area samples. Time was also found to be a factor in the surface area, enough had to be allowed for hydrolysis, but too much resulted in lowering the surface areas. The amount of solvent used was also studied and found to have an important role in the surface area. In samples 8, 10, and 11 it can be seen that decreasing the amount of toluene from 100 to 50 mL had a significant decrease in surface area, going from 786 to 673 m^2/g.

Activation of the Aluminum Oxide (Thermal Dehydration). Aluminum oxide was activated under both argon flow and dynamic vacuum, and it was found that the surface area is significantly higher for samples activated under dynamic vacuum. During activation, the surface area increases, then goes through a maximum, and then decreases. This small decrease in surface area at temperatures above 400 °C can be explained by sintering.

Aluminum Oxide Characterization. By careful characterization of the Al_2O_3 samples it became clear that the NC−Al_2O_3 samples had different textural properties from that of the commercial (CM) Al_2O_3 samples.

Brunauer-Emmet-Teller Method (BET). Commercial Al_2O_3 is most commonly prepared by high-temperature methods, and CM−Al_2O_3 typically had surface areas within the range 100−110 m^2/g. Our NC−Al_2O_3 samples typically possessed surface areas within the range of 790−810 m^2/g after heat treatment at 500 °C. When heated at higher temperatures, the crystallites began to sinter, and surface areas decreased slightly.

Using BET, it was also possible to obtain data on the pore structures (Table 2). The average NC−Al_2O_3 sample after heat treatment possessed pores that were 10 nm in diameter, held 2.05 cm^3/g volume and had a cylindrical pore structure that was open at both ends,

Table 2. Surface Area, Pore Volume, and Diameter of Nanocrystalline Samples Compared to Commercially Available Samples

sample	surface area (m^2/g)	av pore vol (cm^3/g)	av pore diam (nm)
CM−Al_2O_3	103	0.19	7.4
CM−MgO[a]	18.7	0.077	16
NC−Al_2O_3	805	2.1	11
NC−Al_2O_3/MgO[b]	793	1.9	11
NC−MgO	400	0.90	9.0

[a] Also referred to as AP−MgO for aerogel prepared. [b] One mole Al_2O_3 to 1 mol MgO.

as indicated by comparing the shape of the adsorption−desorption curve with standards.

Compressed pellets were prepared of the NC−Al_2O_3 at various compaction pressures and then studied by BET methods to see how the pressure affected the surface area, pore diameter, pore volume, and pore shape. The pressures tested in pounds per square inch (psi) were 2000, 5000, 10000, and 20000. Before being pressed, the samples had about 800 m^2/g surface area, when pressed at 2000 psi the surface area fell to 752 m^2/g, and the area fell to 486 m^2/g at 20000 psi. The average pore diameter also changed with increasing pressure. Before pressing, the samples have 10.8 nm pore openings and did not change much when the samples are pressed at 2000 psi. However, pressing at 20000 psi caused a marked decrease in the size of the pore openings down to 7 nm. Pore volume was also changed with pressure, but not as drastically as the average pore diameter. Before pressing the samples had 2.05 cm^3/g volume, and after being pressed at 2000 psi, the volume dropped slightly to 1.85 cm^3/g, while after pressing at 10000 psi the volume decreased to 1.22 cm^3/g where it generally remained even after being pressed at 20000 psi. The pore shape of the NC−Al_2O_3 sample changed with increasing pressure, according to De Boer's hysteresis. [37] Before any pressure was applied, the sample had a pore structure consisting of cylindrical pores open at both ends; when pressure was applied, this pore structure remained, until 20000 psi, where it was replaced with slit-shaped pores, the space between parallel plates.

X-*ray Diffraction (XRD).* From XRD, we obtained diffraction patterns that showed the NC−Al_2O_3 sample to be less crystalline than the commercial Al_2O_3 samples. The NC−Al_2O_3 had a completely amorphous pattern, due to particle size broadening. [38] From the diffraction patterns the crystallite size of NC−Al_2O_3 could not be determined, even as the temperature was increased. The results show that the NC−Al_2O_3 had a significantly smaller crystallite size than the commercial Al_2O_3 samples; indeed, the average crystallite size for NC−Al_2O_3 activated at 500 °C was very small, less than 2 nm, while the average crystallite size for CM−Al_2O_3 was 19 nm.

Infrared Spectroscopy (IR). The heat-treated samples were ground with KBr, and pressed into pellets. IR spectra taken after heat treatment at 25, 50, 100, 150, 200, 250, 300, 400, and 500 °C indicate a gradual loss of water and a small amount of residual alkoxy groups.

(37) Lowell, S. *Introduction To Powder Surface Area*; John Wiley & Sons: New York, 1979.

(38) Azafoff; Buerger. The Powder Method in X-ray crystallography; McGraw-Hill Book Co.: New York, 1958; Chapter 16.

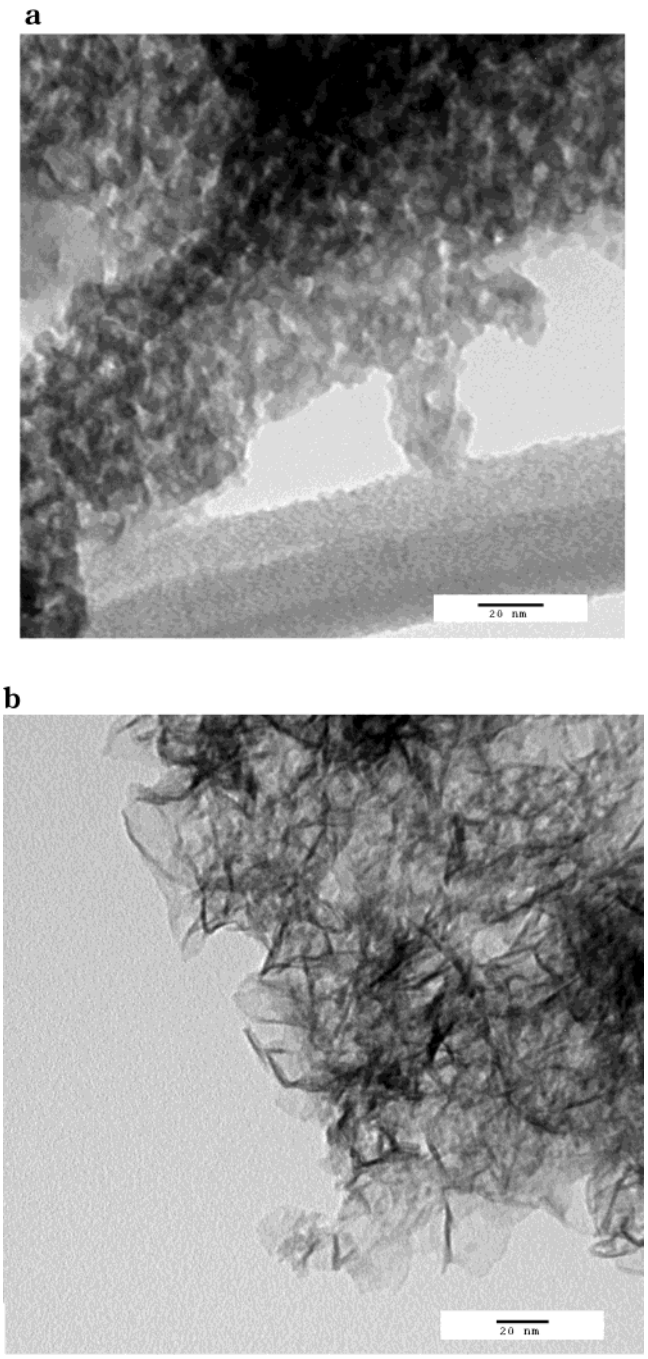

Figure 1. Transmission electron microscope pictures: (a) CM−Al_2O_3; (b) NC−Al_2O_3.

After 500 °C heat treatment, some residual −OH groups remained.

Thermogravimetric Analysis (TGA). Weight loss under nitrogen flow was observed. Total weight loss was about 35% and was found to be the same when conducted in air. Although a gradual loss was observed, most mass loss occurred in the 75−175 and 350−460 °C ranges, which corresponds mainly to surface and internal water loss. These findings are important, since the conversion of $Al(OH)_3$ to Al_2O_3 should yield a 35% weight loss (whereas conversion to AlOOH would be 23%)

Transmission Electron Microscope (TEM). Parts a and b of Figure 1 show TEM photographs, the CM−Al_2O_3 sample exhibited a grainy material with crystallites greater than 10 nm. The NC−Al_2O_3 (Figure 1b) sample

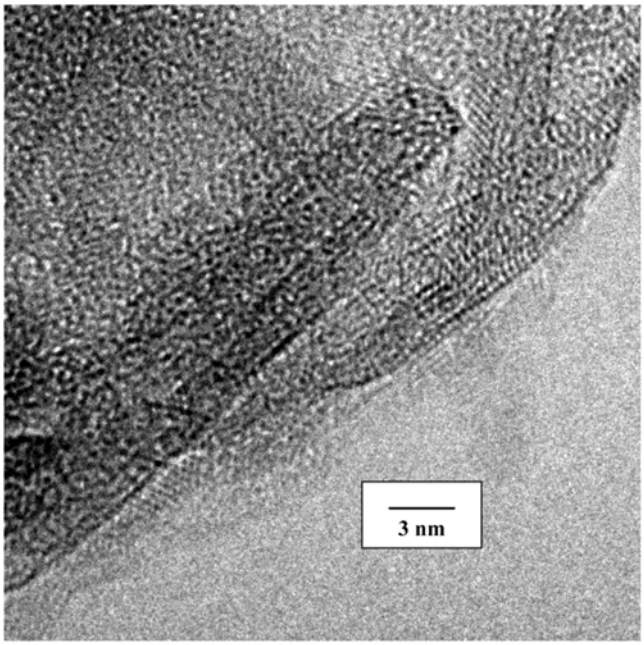

Figure 2. HRTEM of NC−Al_2O_3.

Table 3. Aluminum/Magnesium Oxide Preparation Variables

sample no.	molar ratio Al_2O_3/MgO	amt of solvent (mL)	stirring time (h)	surface area (m^2/g)
1	1/1	20	1	559
2	1/1	70	1	762
3	1/1	120	1	743
4	1/1	70	10	815
5	1/1	70	20	796
6	1/2	70	10	775
7	2/1	70	10	834

consisted of a weblike material, quite different in texture. By compiling data from XRD, TEM, and BET we have concluded that the NC−Al_2O_3 samples are made up of <2 nm crystallites. HRTEM confirmed that the average crystallite size was very small, and the crystals were disordered (Figure 2).

Elemental Analysis. Elemental analysis results for NC−Al_2O_3 preheat-treated to 500 °C under dynamic vacuum gave Al = 47.1% (52.9% calculated for Al_2O_3). These results suggest the presence of some residual OH/H_2O as well as adsorbed CO_2 which was indicated by IR. If CO_2 and surface OH are assumed to be the only adsorbed species, the formula $Al_2O_{2.7}$ $(OH)_{0.53}(CO_2)_{0.03}$ fits the data (oxygen by difference).

Preparation of the Aluminum/Magnesium Oxide. Several experiments were conducted varying the solvent, stirring time, and molar ratios, and all were found to have an effect on the surface area of the resulting sample. Some of the results are shown in Table 3 and demonstrate that the highest surface area was obtained for sample number seven, where a 2:1 Al_2O_3 to MgO ratio was used. For 1/1 Al_2O_3 to MgO samples, time was found to be a factor in the surface area. The amount of solvent (ethanol) used to dilute the water in the hydrolysis step was also found to have an important role in the surface area. In samples 1 and 2, decreasing the amount of ethanol from 70 to 20 mL caused a significant decrease in surface area, going from 762 to 559 m^2/g.

Activation of the Aluminum/Magnesium Oxide (Thermal Dehydration). Aluminum/magnesium oxide was activated under both argon flow and dynamic vacuum, and a small advantage was realized with the vacuum treatment (800 m^2/g using vacuum and 750 m^2/g using argon for 500 °C treatment).

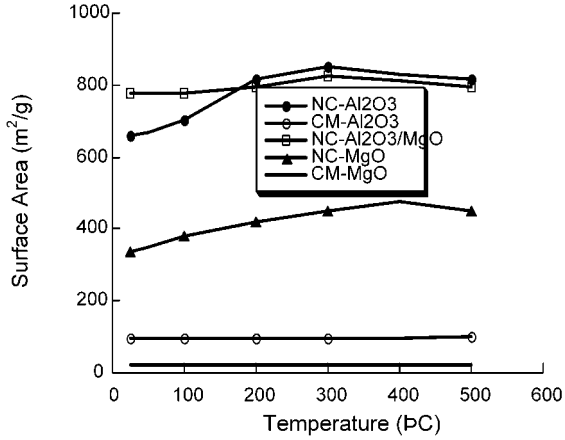

Figure 3. Surface areas of NC−Al_2O_3, CM−Al_2O_3, NC−MgO, CM−MgO, and NC−(1/1)Al_2O_3/MgO upon heat treatment.

(1/1) Aluminum Oxide/Magnesium Oxide Characterization. *Brunauer−Emmet−Teller Method (BET).* The NC−(1/1)Al_2O_3/MgO samples typically possessed surface areas within the range 770−810 m^2/g after heat treatment at 500 °C. Figure 3 shows the heat treatment temperature dependence observed in NC−(1/1)Al_2O_3/MgO compared to NC−MgO, NC−Al_2O_3, CM−Al_2O_3, and CM−MgO. The pore volumes and pore size openings remained very large, comparable to the NC−Al_2O_3 sample and quite different from the NC−MgO and CM samples (Table 2).

Compressed pellets were also prepared of the NC−(1/1)Al_2O_3/MgO heat treated at 500 °C. The pressures employed in pounds/square inch (psi) were the same as those for the Al_2O_3 experiments. Before being pressed the samples had 772 m^2/g surface area, when pressed at 2000 psi the surface area fell to 547 m^2/g, and it fell to 502 m^2/g at 20000 psi. The pore diameter was also affected by pressure: when not pressed the samples had 10.8 nm pores which decreased to 7.8 nm at 2000 psi and then dropped to 6 nm at 20000 psi. Pore volume also changed with pressure, but not as drastically as the diameter or the surface area. Before being pressed the samples had 1.90 cm^3/g volume, while after being pressed at 2000 psi the volume dropped to 0.742 cm^3/g, and then after being pressed at 10000 psi the volume decreased to 0.635 cm^3/g where it generally remained even after being pressed at 20000 psi. The pore shape of the NC−Al_2O_3/MgO sample changed with increasing pressure, according to De Boer's hysteresis,: at first the pore structure consisted of cylindrical pores open at both ends until 10000 psi, where it is replaced with tapered or wedged shaped pores with narrow necks, open at one or both ends.[37] Indeed, these pore structures are different from the NC−Al_2O_3 samples (see earlier results) and quite different from NC−MgO, where pore volumes and pore openings are smaller, and bottleneck and cylindrical pores were observed.[39]

(39) Richards, R.; Li, W.; Decker, S.; Davidson, C.; Koper, O.; Zaikovski, V.; Volodin, A.; Rieker, T.; Klabunde, K. J. *J. Am. Chem. Soc.* **2000**, *122*, 4921.

Table 4. Reaction of Pulses of CCl_4 with Oxide Samples at 500 °C

sample	breakthrough	saturation	molar ratio
NC−Al_2O_3	57	98	1.44 mol of CCl_4:1 mol of Al_2O_3
CM−Al_2O_3	2	17	1 mol of CCl_4:16 mol of Al_2O_3
NC−(1/1)Al_2O_3/MgO	25	88	1.8 mol of CCl_4:1 mol of Al_2O_3/MgO
CM−MgO	1	4	1 mol of CCl_4:32 mol of MgO

[a] Theoretical molar ratio: 1 mol of CCl_4:2 mol of MgO, 1.5 mol of CCl_4:1 mol of Al_2O_3, 2 mol of CCl_4:1 mol of Al_2O_3/MgO. [b] NC−MgO studied at 400 °C.[51]

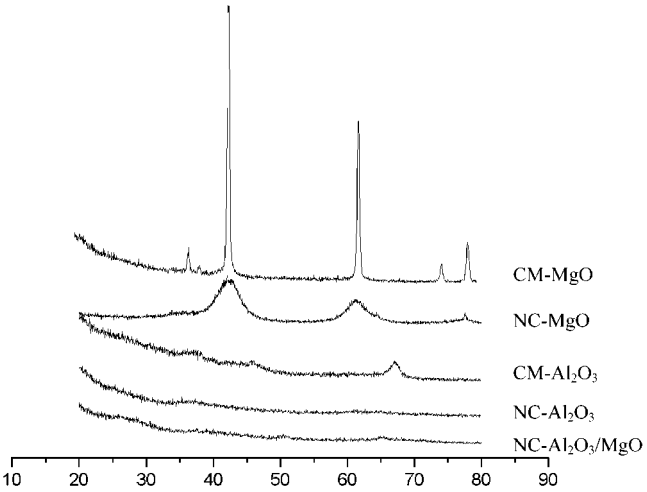

Figure 4. X-ray diffraction patterns for CM−Al_2O_3, CM−MgO, NC−MgO, NC−Al_2O_3, and NC−(1/1)Al_2O_3/MgO.

X-ray Diffraction. Figure 4 compares the XRD pattern for the Mg and Al samples. The Al_2O_3/MgO did not sinter even upon heating to 700 °C.

Infrared Spectroscopy. IR spectra were taken after heat treatment at 25, 100, 200, 300, 400, and 500 °C. A gradual loss of water and solvent was observed from 25 to 500 °C. So when the sample is activated at 500 °C, it can be inferred that there will be a small amount of residual surface −OH present.

Thermogravimetric Analysis. Weight loss under nitrogen flow was about 40% and was found to be the same when conducted in air. There was a gradual weight loss throughout the heating, due to the hydroxide converting to oxide and the removal of the water. The theoretical weight loss is 34%, so the observed 40% indicated that some adsorbed water was also present.

Transmission Electron Microscopy. Figures 1a, 5a, and 5b show TEM photographs, of CM−Al_2O_3, NC−Al_2O_3/MgO, and CM−MgO, respectively. The CM−MgO sample consists of single crystals of varying fairly large sizes. The NC−Al_2O_3/MgO sample however consists of crystallites having an average crystallite size of about 5 nm or smaller, and of quite different morphology from analogous NC−Al_2O_3 and NC−MgO samples.[39]

Elemental Analysis. Elemental analysis results of NC−(1/1)Al_2O_3/MgO preheat-treated to 500 °C under dynamic vacuum were Mg = 13.3% (17% calculated), Al = 30.9% (37.9% calculated), C = 0.65% (0% calculated) and H = 1.2% (0% calculated). Obviously some adsorbed H_2O and CO_2 affected these results (as indicated by IR). The formula $MgAl_2O_{3.3}(OH)_{1.4}(CO_2)_{0.088}(H_2O)_{0.35}$ fits the data (oxygen by difference). It was apparent from TGA that some weakly bound water was present.

Adsorption Studies. *Reaction of Al_2O_3 and (1/1) Al_2O_3/MgO with CCl_4.* The reaction of CCl_4 with Al_2O_3 and Al_2O_3/MgO was carried out to understand the destructive adsorption abilities of the metal oxides toward a model chlorocarbon at elevated temperatures.

$$2\ Al_2O_3 + 3CCl_4 \rightarrow 3CO_2 + 2Al_2Cl_6$$

$$2\ MgO + CCl_4 \rightarrow CO_2 + 2MgCl_2$$

Thermodynamics predicts that the samples containing MgO should be more reactive than the Al_2O_3 samples.[40] However, it will be seen how surface area, crystallite size, and morphology can play an active role.

These reactions were conducted via the pulse method, and the products were identified by GC. The breakthrough injection, saturation injection, and molar ratios are reported in Table 4.

Table 5. Adsorption of SO_2 on Al_2O_3, MgO, and Al_2O_3/MgO Samples at Room Temperature

sample	tot. molecules of SO_2/nm^2 adsorbed	molecules of SO_2/nm^2 physisorbed	molecules of SO_2/nm^2 chemisorbed
NC−Al_2O_3	3.5	1.8	1.7
CM−Al_2O_3	3.5	3.0	0.45
NC−Al_2O_3/MgO	6.8	2.9	3.9
CM−MgO	0.68	0.51	0.17
NC−MgO[35]	6.0	1.5	4.5

Sulfur Dioxide Adsorption on Alumina, and Aluminum/Magnesium Oxide. Adsorption of SO_2 was carried out to learn if the adsorption properties are different for nanocrystals, when compared to commercial microcrystals. Using 19.2 Å^2 as the area of an SO_2 molecule, it can be determined that 5.2 molecules of SO_2/nm^2 would form a monolayer. The experimental results showed that at atmospheric pressure and room temperature, SO_2 adsorbed onto NC−Al_2O_3 up to 3.5 molecules of SO_2/nm^2, similarly on CM−Al_2O_3 there were 3.5 molecules of SO_2/nm^2 adsorbed, and on NC−(1/1)Al_2O_3/MgO there were 6.8 molecules of SO_2/nm^2, whereas on CM−MgO there were only 0.68 molecules of SO_2/nm^2 adsorbed (Table 5). These data indicate that NC−Al_2O_3/MgO efficiently adsorb SO_2 in slightly more than one layer. After adsorption had ceased, the samples were subjected to dynamic vacuum for 100 min to remove the physisorbed species. After this vacuum treatment, there remained 1.70 and 0.45 molecules of SO_2/nm^2 present chemisorbed onto the NC−Al_2O_3, and CM−Al_2O_3 samples, respectively. The vacuum treatment removed most of the adsorbed SO_2 from the CM−MgO, whereas the NC−Al_2O_3/MgO sample retained 3.9 molecules of SO_2/nm^2.

Next, an in situ IR study was performed to help identify how the SO_2 was binding.[41] This setup allows IR spectra to be obtained of the exact same spot before SO_2, with SO_2, and after evacuation of SO_2. The study was conducted at room temperature with 20 Torr of SO_2.

(40) Barin, I.; Knacke, O. *Thermochemical Properties of Inorganic Substances*; Springer-Verlag: Berlin, 1973.

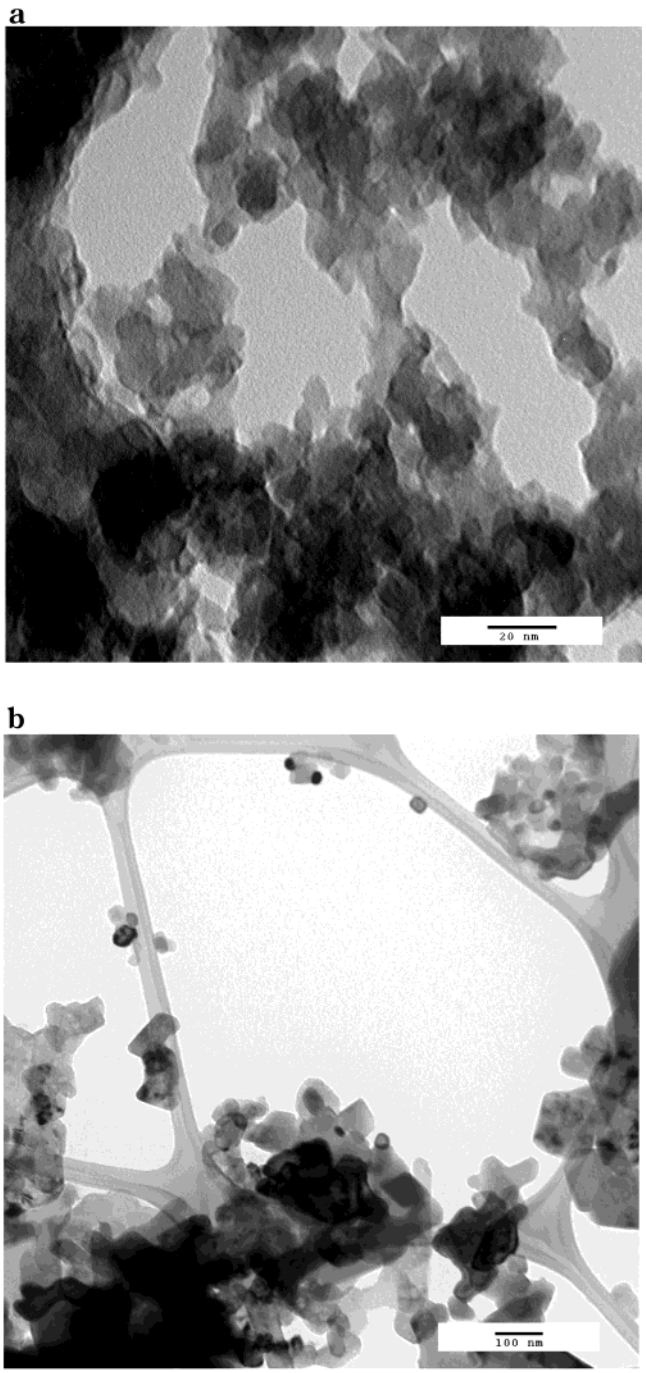

Figure 5. Transmission electron microscope pictures: (a) NC−Al_2O_3/MgO; (b) CM−MgO.

Figure 6 shows the spectra after a 2 h evacuation for all four samples. Both CM−MgO, and CM−Al_2O_3 showed no adsorbed species. Both NC−Al_2O_3 and NC−Al_2O_3/MgO show new peaks at 1135 and 1330 cm^{-1} that correspond to chemisorbed monodentate SO_2 adsorbed species.[35,42−46] These results indicate that the NC samples have a high capacity for chemisorption of SO_2 (Table 5) per unit surface area, indicating an intrinsically higher activity.

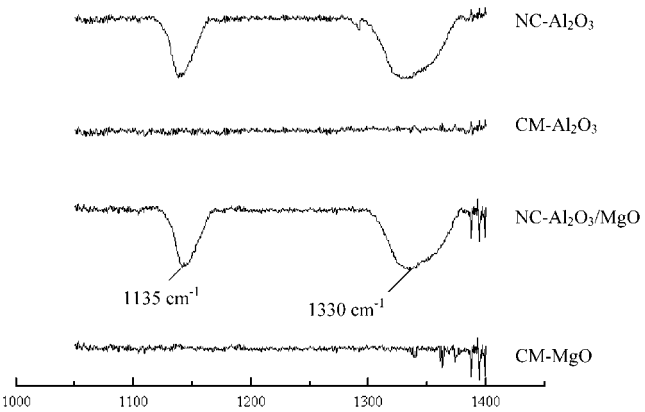

Figure 6. IR spectra after 2 h evacuation at room temperature.

Table 6. Destructive Adsorption of Paraoxon in Pentane on the Oxide Powders

sample	molar ratio
NC−Al_2O_3	1 mol of Paraoxon:11 mol of Al_2O_3
CM-Al_2O_3	1 mol of Paraoxon:63 mol of Al_2O_3
NC−(1/1) Al_2O_3/MgO	1 mol of Paraoxon:5.6 mol of Al_2O_3/MgO
CM−MgO	1 mol of Paraoxon:188 mol of MgO
NC−MgO	1 mol of Paraoxon:46 mol of MgO

Destructive Adsorption of Diethyl 4-Nitrophenyl Phosphate (Paraoxon). The adsorption of Paraoxon was carried out to compare the rates and capacities for the metal oxide samples to dissociatively chemisorb a polar organic, more specifically a toxic insecticide. By monitoring of the disappearance of an UV band for Paraoxon in pentane, the data shown in Table 6 were obtained, and the results are striking. Neither of the CM samples adsorbed much Paraoxon, while the NC samples rapidly adsorbed the entire sample and developed a bright yellow color, indicating the likely formation of the *p*-nitrophenoxide anion on the surface.

Additional experiments with larger and larger amounts of Paraoxon were studied, and it was found that about 5.5 μL of Paraoxon (2.55×10^{-5} mol, 1.54×10^{19} molecules) was adsorbed by 0.0300 g of NC−Al_2O_3, and about 9.5 μL of liquid Paraoxon (4.40×10^{-5} mol, 2.65×10^{19} molecules) was taken up by 0.0350 g of NC−Al_2O_3/MgO. One molecule of Paraoxon dissociated and with the *p*-nitrophenoxide lying flat would occupy about 1 nm^2 of surface area. In a 0.0300 g sample of NC−Al_2O_3 2.4×10^{19} nm^2 surface area is available, and so we can estimate that about 0.77 monolayer is adsorbed under these conditions. In a 0.0350 g sample of NC−Al_2O_3/MgO 2.8×10^{19} nm^2 surface is available, and so we can estimate that about 1.04 monolayers are adsorbed under these conditions (room temperature, 0.01 M concentration in pentane).

After the reaction was complete, the powders were filtered, and IR studies were done on the solids. The results from the IR show that the NC samples have many new species adsorbed to the powder, whereas the CM samples have little if any new species adsorbed. Table 7 gives IR spectra assignments for free Paraoxon and for adsorbed Paraoxon which are based on the literature.[33,41,42,47,48] According to IR spectra taken following the reaction with Paraoxon for CM−Al_2O_3, NC−

(41) Koper, O. Properties of High Surface Area Calcium Oxide and its Reactivity Towards Chlorocarbons. Ph.D. Thesis, Kansas State University, 1996.
(42) Stark, J. V.; Klabunde, K. J. *Chem. Mater.* **1996**, *8*, 1913−1918.
(43) Goodsel, A. J.; Low, M. J. D.; Takezawa, N. *Environ. Sci. Technol.* **1972**, *6*, 3, 268.
(44) Dunn, J. P.; Koppula, P. R.; Stenger, H. G.; Wachs, I. E. *Appl. Catal., B* **1998**, *19*, 103.
(45) Stark, J. Characterization and Studies of Reactivity of Magnesium Oxide. M.S. Thesis, Kansas State University, 1995.
(46) Li, Y.; Schlup, J.; Klabunde, K. J. *Langmuir* **1991**, *7*, 1388.

Table 7. FTIR Bands for Free and Adsorbed Paraoxon

free Paraoxon	assignment	adsorbed Paraoxon	assignment
860	ν(C−N)	860	ν(C−N)
930	CH_3 rock	930	CH_3 rock
1045	ν(Et-O−(P))	1045	ν(C−O−(P))
1107	CH_3 rock	1107	CH_3 rock
1164	CH_3 rock	1164	CH_3 rock
1232	ν(P−O−(Ar))		
1296	ν(P═O)	1313	ν(P═O)
1348	ν_s(N−O)	1348	ν_s(N−O)
1491	ν(C−C ring)	1491	ν(C−C ring)
1526	ν_{as} N−O	1526	
1593	ν(C−C ring)	1593	ν(C−C ring)

Al_2O_3, CM−MgO, and NC−(1/1)Al_2O_3/MgO, there was some change when Paraoxon was adsorbed. A band at 1296 cm^{-1} assigned to ν(P═O) was broadened and shifted to approximately 1313 cm^{-1}. Also, the original peak for free Paraoxon at 1232 cm^{-1} assigned to the ν(P−O−Ar) stretch had disappeared. The band due to ν(P−O−Et) at 1045 cm^{-1} did not change much (see Table 7), suggesting that the EtO−P moieties were not perturbed or destroyed. We tentatively conclude from these data that P═O bond is strongly perturbed through binding to Lewis acid sites on the Al_2O_3 and MgO surfaces and that the P−OAr bond is broken.

Discussion

The modified aerogel procedure employed is designed to yield high quality gels under rapid gelation conditions.[49] Solvent-to-alkoxide ratios are important as well as the solvent choice. The addition of toluene has at least two effects; lowering viscosity and polarity. This in turn, causes a more rapid hydrolysis step and faster gelation, which results in a more "open" structure.[49] After supercritical drying[50] very high surface area Al-$(OH)_3$ or mixed $MgAl(OH)_4$ were obtained. Subsequently, after dehydration of the hydroxides, high surface area oxides with large pore volumes were obtained.

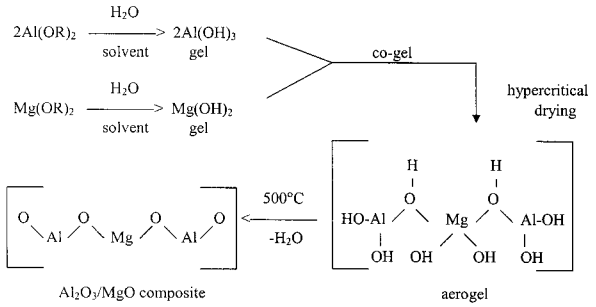

This synthetic approach is very different from earlier reports, where reactive sputtering,[12] dc arc plasmas,[13] crysol techniques,[14] and related sol−gel methods were used.[16,17] For example Ramesh and co-workers[17] used aluminum triisopropoxide as a starting material in a sol−gel synthesis and obtained amorphous Al_2O_3, surface area 97−183 m^2/g, much lower than the Al_2O_3 samples reported herein.

Earlier work on mixed Al_2O_3/MgO systems dealt with impregnating Al_2O_3 with magnesium salts followed by heat treating; surface areas of 136−184 m^2/g were reported.[32] In addition, Chi and Chang report that Al_2O_3 impregnated with MgO could adsorb more NO at 523 K than did a series of other similar compositions.

It should be emphasized that the modified aerogel procedure reported herein is intended to prepare MgO−Al_2O_3 in molar ratios of 1:1 or other desired ratios. The point is to obtain intimately intermingled mixtures, essentially molecular in nature, and gain advantages by obtaining higher surface areas of the more reactive component throughout the structure, in this case MgO (more basic in nature) with Al_2O_3 (which supports very high surface areas).

Thus, the so obtained Al_2O_3 and Al_2O_3/MgO materials reported herein are higher in surface area than materials reported before, and remarkably thermally stable (with minimal sintering even as high as 700 °C) and are essentially amorphous or at least have crystal domains 2 nm or less. Most importantly, the chemical adsorptive properties of these materials are remarkable.

There are three features of nanocrystalline materials that affect their chemical reactivities: (1) high surface areas, meaning large surface-to-bulk ratios; (2) unusual morphologies; (3) crystal disorder.[39,51−53] All three of these features are present in materials at hand, as their high chemical reactivity has demonstrated. In fact, these ultrafine powders behave as stoichiometric reagents in some reactions, such as CCl_4 destructive adsorption.

In surface adsorption processes, such as with SO_2 and Paraoxon, very large capacities are realized due to both surface area and enhanced surface reactivity. Note the amounts adsorbed normalized for surface areas (Tables 5 and 6).

An additional interesting feature for the mixed sample Al_2O_3/MgO is that the reactivity of this material is superior to NC−Al_2O_3. This is probably due to the greater Lewis basicity of the MgO present, which should be and is beneficial for adsorption of the acid gas SO_2 (see Table 5). This effect is also evident in the Paraoxon adsorption results (Table 6) where considerably higher adsorption capacity was realized.

These results indicate that the NC−Al_2O_3/MgO mixed product has enhanced chemical reactivity properties over NC−Al_2O_3 or NC−MgO. This is an advantageous result and must be due to the Lewis base nature of MgO being preserved while maintaining the large pore volume and large surface area of the Al_2O_3 partner. This suggests that intimate commingling of many other nanocrystalline oxides could provide enhanced reactivities, in a sense tailored to the desired properties.

Acknowledgment. The support of the National Science Foundation and the Army Research Office are acknowledged with gratitude.

CM011590I

(47) Lin-Vien, D.; Colthup, N.; Fateley, W.; Grasselli, J. *The Handbook of Infrared and Raman Characteristic Frequencies of Organic Molecules*; Academic Press: New York, 1991.

(48) Pretsch, E.; Clerc, T.; Seibl, J.; Simon, W. *Tables of Spectral Data for Structure Determination of Organic Compounds*; Springer-Verlag: New York, 1989.

(49) Diao, Y.; Walawender, W.; Sorenson, C. M.; Klabunde, K. J. *Chem. Mater.* **2002**, *14*, 362.

(50) (a) Kistner, S. S. *J. Phys. Chem.* **1932**, *36*, 52. (b) Teichner, S. J.; Nicolaon, G. A.; Vicarini, M. A.; Gardes, G. E. E. *Adv. Colloid Interface Sci.* **1976**, *5*, 245.

(51) Decker, S.; Lagadic, I.; Klabunde, K. J.; Michalowicz, A.; Moscovici, J. *Chem. Mater.* **1998**, *10*, 674.

(52) Itoh, Utamapanya, S.; Stark, J. V.; Klabunde, K. J.; Schlup, J. *Chem. Mater.* **1993**, *5*, 71.

(53) Jiang, Y.; Decker, S.; Mohs, C.; Klabunde, K. J. *J. Catal.* **1998**, *180*, 24.